

# Extrusion freeforming of ceramics through fine nozzles

Imen Grida<sup>1</sup>, Julian R.G. Evans\*

*Department of Materials, Queen Mary, University of London, Mile End Road, London E1 4NS, UK*

Received 28 January 2002; accepted 12 May 2002

## Abstract

Thermoplastic suspensions of 55 vol.% zirconia in a wax-based vehicle were extruded through a range of fine nozzles with diameters from 76 to 510  $\mu\text{m}$ . Fixed pressure extrusion under a maximum nitrogen gas pressure of 350 kPa and an extrusion temperature of 175 °C were used. The ability of unfiltered suspensions to flow in fine nozzles depended critically on the mixing method. Ceramic latticework in the form of structures suitable for bone substitute scaffolds were created by extrusion freeforming, a process also known as fused deposition modelling (FDM) or fused deposition of ceramics (FDC). However, precisely ordered deposition could not be obtained by fixed pressure extrusion with a 55 vol.% suspension because of rate variations due to slight mixing inhomogeneities. The quality of welds was examined. Heat transfer considerations show that the use of thermoplastic suspensions is not ideal for fine (< 100  $\mu\text{m}$  dia.) filament work because the fibres solidify before folding and welding.

© 2002 Elsevier Science Ltd. All rights reserved.

*Keywords:* Extrusion freeforming; Fused deposition; Latticework;  $\text{ZrO}_2$

## 1. Introduction

Creating an artefact from a cylindrical strand of deformable ceramic has its origin in Egypt in the Naqada 1 period (ca 4500–4000 BC) from where there is evidence of coiled clay pots.<sup>1</sup> In modern times, a range of solid freeforming processes, each with a separate designation are based on the same principle. The names include fused deposition modelling (FDM), multiphase jet solidification (MJS), fused deposition of ceramics (FDC) and extrusion freeforming (EFF). The last of these provides quite a good descriptive title for the whole set of processes. Solid freeforming can be defined as the creation of a shape by point, line or planar addition of material without confining surfaces other than a base. The methods can thus be classified dimensionally and extrusion freeforming is in the group of linear methods.

In fused deposition modelling, a polymer filament, often acrylonitrile butadiene styrene, is fed into a heated extrusion head and deposited in paths defined by the

two-dimensional sub-images of a three dimensional CAD file shape.<sup>2</sup> A complex shape can be created without confining surfaces. Glass<sup>3</sup> and liquid crystal<sup>4</sup> reinforced polymers have also been used. Precise temperature control is needed ( $\pm 0.5$  °C) and dimensional accuracy rests on the use of shrinkage compensation factors<sup>5,6</sup> and optimised deposition strategies.<sup>7,8</sup>

In multiphase jet solidification,<sup>9–11</sup> a ceramic or metal powder suspension, in a wax or polymer vehicle or indeed, a semisolid metal, is extruded onto the building platform by a nozzle whose discharge rate is matched to the 3-axis table travel. The integration of this with other prototyping techniques provides a route for small production runs of ceramics.<sup>12</sup>

A similar technique (FDC) has been used to make structural ceramics<sup>13</sup> and piezoelectric ceramics for incorporation into ceramic-polymer composites both directly<sup>14</sup> and indirectly by first making a disposable mould.<sup>15</sup> Typically the filament diameter was 1.8 mm.<sup>16</sup> The method has been extended to accommodate more than one material (fused deposition of multi-materials: FDMM) and hence to make photonic bandgap structures<sup>17</sup> and piezoelectric actuators with novel configurations.<sup>18</sup>

Likewise, extrusion freeforming<sup>19</sup> can be used for ceramic prototypes; a 25 gauge hypodermic needle was used (i.d. 250  $\mu\text{m}$ ) for the preparation of nylon 6 parts

\* Corresponding author.

*E-mail address:* j.r.g.evans@qmul.ac.uk (J.R.G. Evans).

<sup>1</sup> Present address: Department of Industrial Engineering, Ecole National d'Ingénieur de Tunis, Tunisia.

by extrusion of liquid monomer.<sup>20</sup> State change occurs by polymerisation on a heated substrate. This is one of several approaches for avoiding the dependence on solidification and is relevant to the results of the present work.

As with most solid freeforming processes there is a balance to be struck between the resolution of the point, line or plane that is being deposited and the rate of building. The ability to extrude through a range of nozzles with different diameters offers the opportunity to improve both. Thus fine nozzles can be brought into play in the region of complex design while larger nozzles are used for regular sections.<sup>21</sup>

Again, most solid freeforming processes produce surfaces with ripples, steps or striations. Applications where this is not a drawback include scaffolds in tissue engineering or in bone-substitute and ceramic preforms for metal matrix composites. Porous calcium phosphate ceramics are used to encourage post operative bone growth both in dentistry<sup>22</sup> and in orthopaedic surgery.<sup>23</sup> Calcined mammalian bone, coral or ceramics made by a range of foaming techniques can be used. These offer little control of pore size, pore size distribution or ceramic volume fraction. The creation of ceramic or polymer latticework by extrusion freeforming to give variations on the ‘log-pile’ structure provides these features as well as the capability to use ceramics of well-defined purity. Furthermore, the characteristic weakness in FDM of rippled walls is absent.

One of the ways to prepare metal matrix composites takes a fibre preform, typically of alumina and infiltrates it with an aluminium alloy by squeeze casting. The importance of the contiguity of reinforcement and of ductile matrix is emphasised<sup>24</sup> and methods that produce bicontinuous composites are sought, for example by making preforms from foams<sup>25</sup> or fibre bundles.<sup>26</sup> The connections between fibres in a three dimensional network are considered to<sup>27</sup> influence composite properties.

Provided extrusion freeforming could be adapted to discharge through very fine nozzles, fibre preforms could be designed to a specification produced, for example by topological optimisation methods.

An extrusion freeforming approach to scaffolds has already been explored for dilute (7 vol.%) suspensions of ceramics in polymers.<sup>28,29</sup> Hutmacher and co-workers<sup>28</sup> have extruded such suspensions of hydroxyapatite in polycaprolactone to give 0°–60°–120° lay-ups using 0.41 and 0.25 mm diameter dies. In-vitro studies with human fibroblasts and periosteal cells showed that extra-cellular matrix was produced within one week and the structure was completely filled with cellular tissue in 3–4 weeks.<sup>29</sup>

It was with these thoughts in mind that the present work was undertaken to examine the issues of mixing, nozzle refinement and filament weldability in this process. Rather than use a calcium phosphate-based ceramic, a

Table 1  
Composition of ceramic suspension

Constituent	Density (kg m <sup>-3</sup> )	Weight (%)	Volume (%)
Zirconia	6000	88.9	55
Microcrystalline wax	905	7.2	30
Stearic acid	941	3.9	15

zirconia-wax system of well-characterised viscosity was chosen for a pilot study.

## 2. Experimental details

The ceramic powder was a 5 wt.% yttria-doped zirconia, HSY3 (*ex* Daiichi-Kigenso, Japan) and was incorporated in a blend of stearic acid (GPR, *ex* BDH-Merck Ltd, Lutterworth, Leics., UK) and microcrystalline wax (Okerin 1865H *ex* Astor chemicals, West Drayton, UK) at 55 vol.%.

The composition is given in Table 1. Mixing was carried out on a twin roll mill (Joseph Robinson and Co. Ltd, Manchester, UK) at 100 °C for 15 min. Further mixing was carried out on a part of this batch by dissolving it in octane at approximately 1:20 dilution and passing it through the chamber of high energy bead mill (type KDLA Dyno-mill, Glen Creston, Stanmore, UK) charged with 0.5 mm diameter zirconia media (*ex* Tosoh, Tokyo, Japan). The mixture was dried, granulated and vacuum treated to remove residual solvent.

The extruder head was mounted on a three-axis table (Parker Hannifin plc, Poole, Dorset, UK) driven by ‘Easi-tools’ software. The set-up is shown in Fig. 1. The extruder was heated by a purpose-built band heater (Elmatic Ltd. Cardiff, UK) and pressure was supplied by an oxygen-free nitrogen cylinder fitted with a 1 MPa regulator.

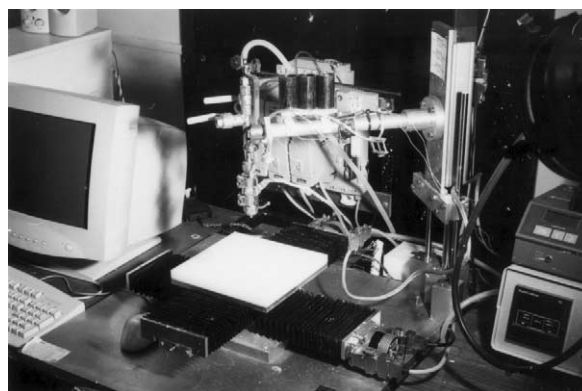


Fig. 1. The extrusion freeforming apparatus with three axis table and extruder mounted on the z axis.

Table 2  
Details of nozzles

Diameter/ $\mu\text{m}$	Description	Code	Source
510	Hypodermic needle	21g	Kaycee Veterinary Products Ltd, Lindfield, UK.
410	Hypodermic needle	22g	Kaycee Veterinary Products Ltd, Lindfield, UK.
254	Seamless stainless steel tube	T321	Accles and Pollock Ltd, Warley, UK
191	Sapphire nozzle	INZA0705014K	Lee Products Ltd, Gerrards Cross, UK
100	Sapphire nozzle	INZA0402054K	Lee Products Ltd, Gerrards Cross, UK
76	Sapphire nozzle	INKA2437210H <sup>a</sup>	Lee Products Ltd, Gerrards Cross, UK

<sup>a</sup> Valve mechanism removed leaving sapphire nozzle mounted in tube.

Details of the nozzles are given in Table 2. These were fitted into a brass holder. The table was programmed to produce a lattice of successive orthogonal layers (a so-called log-pile structure). The finished structures were heated in flowing air on a ramp: 60 °C/h to 150 °C, 5 °C/h to 400 °C, 1 h dwell. For the 76  $\mu\text{m}$  fibre, the second ramp was 10 °C/h. They were sintered on a bed of coarse alumina at 10 °C/min to 1500 °C and held for 2 h. Microscopic examination was done on a field emission scanning electron microscope (model 6300F, Jeol, Japan). The dimension scale was calibrated with a SIRA test specimen (A316, 19.7 lines/mm *ex* Agar Scientific, Stanstead, UK).

### 3. Results and discussion

This composition (Table 1) has been devised for the injection moulding of fine zirconia powders<sup>30</sup> and the flow behaviour of closely related suspensions (60 vol.% HSY3 zirconia) has been examined and is shown in reference 31. During extrusion through the 100  $\mu\text{m}$  diameter die, the apparent wall shear rate was in the region of 1000  $\text{s}^{-1}$  with the extrusion rate at 10  $\text{mm s}^{-1}$  and the wall shear stress was about  $2 \times 10^4$  Pa. This apparent viscosity of 20 Pa s is too low when compared with the data in reference 27 even taking into account the lower ceramic volume fraction. Clearly there are three issues to consider in the flow of crowded suspensions in very fine, short nozzles where the surface to volume ratio ( $2/r$ ) is high ( $4 \times 10^4 \text{ m}^{-1}$ , in this case). First there is a contribution to mass transport by wall slip known to occur in ceramic suspensions,<sup>32</sup> secondly there is a contribution to higher wall shear rate made by segregation of powder from the wall to the bulk.<sup>33</sup> These are distinct effects because wall slip occurs in unfilled polymer melts. Both these effects dramatically change the velocity profile across the nozzle from parabolic to plug flow. Thirdly there are end effects associated with elongational flows particularly at the entrance.<sup>34</sup> This is an area of the rheology of crowded suspensions deserving attention and the questions of instrument design, notably the achievement of steady flows at low speeds in such rheometers is central to the acquisition of valid flow data applicable to very fine capillaries.

The scope of this work is to explore the materials and equipment issues involved in creating very fine sintered ceramic lattices by an extrusion freeforming method. The free extrusion cylinder does not give adequate control of rate and so ordered lattices are not easily made by this approach. An example of a sintered lattice is shown in Fig. 2 and the structure of the welds is discussed below.

These experiments do throw light on the specifications to be demanded of a stepper-driven extruder head. The design equation is:

$$V_r = \frac{L}{t_c} = \left(\frac{r}{R}\right)^2 V_e \quad (1)$$

where  $V_R$  and  $V_e$  are the velocities and  $R$  and  $r$  are the radii of the ram and extrudate respectively,  $t_c$  is the cycle time before recharging the barrel and  $L$  is the ram displacement.

The present work suggests that a 76  $\mu\text{m}$  diameter nozzle can easily be used for unfiltered ceramic extrusion and hence that a 50  $\mu\text{m}$  diameter nozzle is likely to deliver extrudate provided filtration is deployed against entrained debris. With  $r = 25 \mu\text{m}$  and  $V_e = 5 \text{ mm s}^{-1}$ , the volumetric flow rate is only  $10^{-11} \text{ m}^3 \text{ s}^{-1}$ . To accommodate sufficient charge for  $t_c = 8000\text{s}$  in a ram extruder,

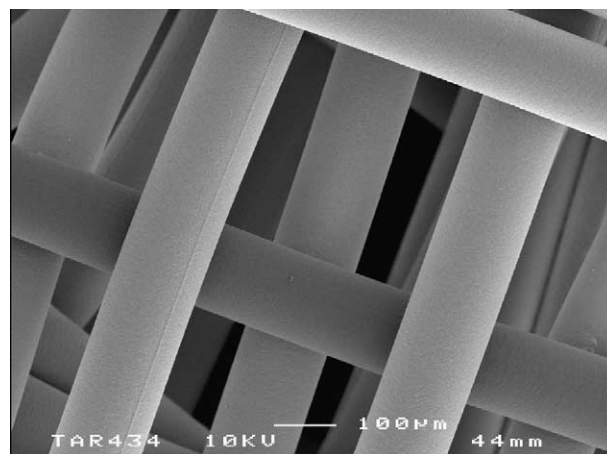


Fig. 2. Sintered lattice of zirconia—the irregularity is due to inconsistent extrusion rate from a constant pressure extruder.

the barrel capacity should be  $8 \times 10^{-8} \text{ m}^3$ . Given a reasonable maximum lead-screw displacement of  $L = 50 \text{ mm}$ , a 1.4 mm diameter barrel is needed and the ram velocity,  $V_R$  would need to be  $6 \mu\text{m s}^{-1}$ . Thus substantial reduction gearing or micro-stepping may be needed to prevent the step size giving pulsed extrusion. Fortunately, modern high ratio reduction gearboxes are available that are almost free from backlash. Innovative drive mechanisms such as the piezoelectric inch-worm may be called for. Obviously  $V_R$  scales with  $r^2$  and so this problem only emerges in attempts to extrude single fine threads for a long time. The use of a miniature screw extruder also introduces problems of irregular rate of discharge and has not been explored here.

In these experiments, the suspensions that were mixed by twin screw extrusion alone, could pass continuously through the 510  $\mu\text{m}$  nozzle but experienced frequent blockages when the 410  $\mu\text{m}$  nozzle was tested. The same suspension, after milling in octane and thorough drying, passed easily without filtration through all the nozzles tried. Its lower limit is thus below 76  $\mu\text{m}$  diameter. This result points to the presence of residual unbroken agglomerates in the extruded material.

Various methods were used to detect these including dilution of the suspension and observation using the back-scattered electron image and the careful study of fracture surfaces of the wax-based suspensions. It was not possible to obtain representative images that showed an unambiguously higher incidence of large agglomerates in either mixture. Many techniques can be applied to assess agglomeration in filled systems<sup>35</sup> of which electron microscopy is one of the more reliable. Thus we are not in a position to offer direct evidence that the extrusion performance after milling was due to agglomerate destruction but the effectiveness of the severe milling operation suggests that it was so.

The inconsistent rate obtained from the fixed pressure extrusion cylinder is evidence of slight mixing inhomogeneities because at high powder loadings viscosity is very sensitive to ceramic volume fraction.<sup>36</sup> The scale of mixing can be defined as the smallest volume above which homogeneity prevails. The extrudate velocity  $V_e$ , was generally stable over an 80 mm strand length of 76  $\mu\text{m}$  diameter thread having a volume of  $4 \times 10^{-10} \text{ m}^3$  (equivalent to a sphere of radius 440  $\mu\text{m}$ ) suggesting that mixing was uniform in that volume. This provides an estimate of the scale of mixing.

The extruder barrel was constructed of brass for ease of machining. Evidence both of dezincification and green discoloration of the material lining the barrel indicated a reaction with the stearic acid during prolonged heating at 175 °C. Similarly, the epoxy resin adhesive used in the construction of the nozzle plates began to degrade at this temperature and on one occasion a nozzle was ejected onto the building platform.

These are matters that can be addressed by attention to materials selection and equipment design but a fundamental problem has also come to light in these experiments. Extrusion freeforming, as in other solid freeforming methods requires a change of state. In stereolithography, this is achieved by photo-polymerisation, in selective laser sintering and fused deposition modelling by solid-liquid phase change and in ink-jet printing by evaporation of solvent. In extrusion freeforming, the filament is required to travel a short distance from the nozzle, fold and weld to the previous layer on the building platform. If it has cooled before making contact with the previous layer, the welds are insufficiently strong and if it has cooled before folding then it cannot even make contact and freeforming is not possible. This was the case with the 76  $\mu\text{m}$  diameter strands. They would neither fold nor weld. The use of a hot air tube from a soldering station or a radiant heater did not ameliorate this situation.

The unsteady state cooling of a cylindrical strand from its processing temperature ( $\theta_1 = 175 \text{ °C}$ ) to its solidification point ( $\theta = 60 \text{ °C}$ ) in ambient conditions ( $\theta_0 = 20 \text{ °C}$ ) is sensitive to radius. Taking the thermal conductivities ( $\lambda$ ) of ceramic and organic vehicle as 2 and 0.25  $\text{Wm}^{-1} \text{K}^{-1}$  respectively and using Maxwell's equation which has been shown to be valid for ceramic suspensions<sup>37</sup>

$$\lambda^* = \lambda_2 \frac{(1 + 2V_1)\lambda_1 + 2(1 - V_1)\lambda_2}{(1 - V_1)\lambda_1 + (2 + V_1)\lambda_2} \quad (2)$$

where subscripts 1 and 2 refer to ceramic and organic vehicle respectively, the composite conductivity ( $\lambda^*$ ) is  $0.7 \text{ Wm}^{-1} \text{K}^{-1}$ . The specific heat is  $670 \text{ J kg}^{-1} \text{K}^{-1}$  found from the gravimetric law of mixtures (using  $C_{p1} = 400 \text{ J kg}^{-1} \text{K}^{-1}$  and  $C_{p2} = 2900 \text{ J kg}^{-1} \text{K}^{-1}$ ) and the density is  $3700 \text{ kgm}^{-3}$  from the volumetric law of mixtures. This gives the composite thermal diffusivity  $\alpha^* = \lambda^*/C_p^*\rho^* = 2.8 \times 10^{-7} \text{ m}^2 \text{ s}^{-1}$ . In static air, the surface heat transfer coefficient is approximately  $13 \text{ Wm}^{-2} \text{K}^{-1}$ <sup>38</sup> from which the time for the temperature at the core to reach the solidification temperature can be found using Heisler charts<sup>39</sup> and the approximation for low Biot number. The data are shown in Table 3 and they indicate that the thread extruded from the 76  $\mu\text{m}$  diameter nozzle is fully solidified in less than 5 s.

Table 3

Unsteady state solidification times for the filament core ( $\lambda^* = 0.72 \text{ Wm}^{-1} \text{K}^{-1}$ ,  $C_p^* = 700 \text{ J kg}^{-1} \text{K}^{-1}$ ,  $\rho^* = 3713 \text{ kg m}^{-3}$ )

Diameter/ $\mu\text{m}$	Biot number/ $10^{-3}$	Solidification time/s
500	4.5	30
190	1.7	11
75	0.7	5
50	0.5	3

The requirements of this linear building process are that the extrudate should (a) deform to follow the intended path and to settle on the previous layer, (b) bond to the previous layer and (c) change its state. The methods available for state change are limited; solidification, polymerisation, crosslinking or evaporation of solvent are the main possibilities. For the fine filament work described here it is clear that solidification is not ideal. Solvent evaporation offers more scope for control. When the milled mixture was diluted with octane until it would pass through the nozzles at 40 °C, there was a longer time for state change due to evaporation. Both the rate of evaporation and the rate of diffusion through the suspension are strongly influenced by the molecular mass of the diffusant. The present composition is therefore ideal for systematic experiments on a solvent-based system using a wide range of non-toxic paraffinic diluents.

Fig. 3 shows a zirconia fibre extruded through a 76 µm sapphire nozzle and sintered to give a final diameter of 65 µm. The nominal linear shrinkage was 14%.

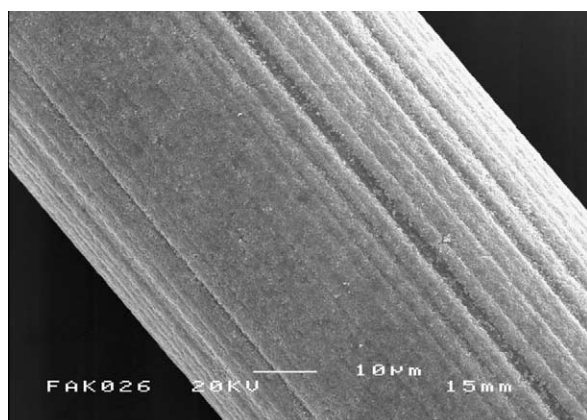


Fig. 3. Sintered zirconia fibre of diameter 65 µm prepared from bead milled suspension extruded through a 76 µm diameter sapphire nozzle.

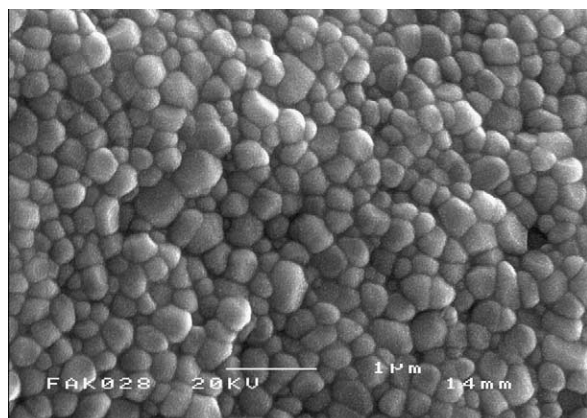


Fig. 4. Sintered surface of a 65 µm diameter zirconia fibre.

Although the surface contains striations arising from the die profile, the sintered surface (Fig. 4) is uniform and displays an average grain size in the 0.4 µm region. These fibres cannot be freeformed because they tend to solidify before folding and welding but the extrudate from the 190 µm sapphire die could be freeformed. An example is shown in Fig. 5. The extent of welding is not great and the wall retains the steps typical of freeformed artefacts but much exaggerated by the failure of a highly filled suspension to coalesce. This is partly due to the high yield stress<sup>31</sup> and partly due to the rapid cooling of highly filled materials.<sup>37</sup> Fig. 6 shows part of a log-pile structure assembled from 100 µm diameter fibres that has been sintered and then fractured. Again the linear shrinkage is 14%. The weld areas are quite small and there was very little distortion of the circular section of the fibres at the weld site. The time available for coalescence at the circular junction between fibres is also related to the method of state change. Thermoplastic systems seem to provide insufficient time for fine threads.

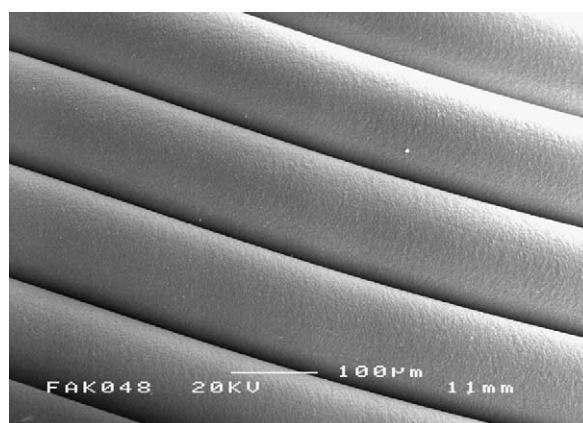


Fig. 5. Sintered wall constructed from welded zirconia filament from a 190 µm die. Although a weld forms, it is limited to the proximity of the contact line and the cylindrical section of the filaments is largely preserved.

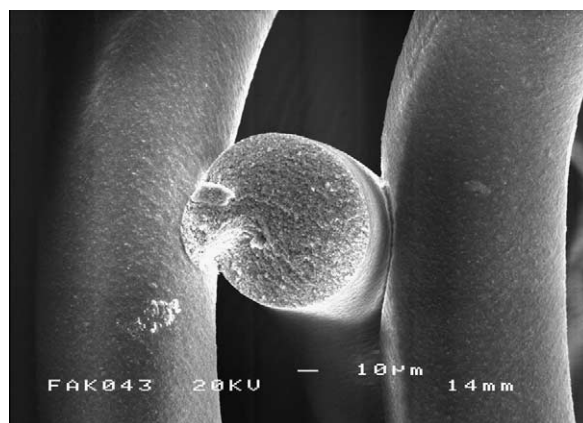


Fig. 6. Fracture of a sintered zirconia "log-pile" structure made from a 100 µm diameter sapphire nozzle. The weld area is small and the fibres are relatively undistorted.

#### 4. Conclusions

It seems reasonable to conclude from this pilot study that highly filled ceramic suspensions can be extruded through fine (<100 µm dia.) nozzles. The smallest sapphire nozzle available was 76 µm and continuous operation was possible; the lower limit has not been found. High energy bead milling was needed to achieve this. The use of a high shear twin screw extruder did not provide a suspension that would pass continuously through nozzles less than 510 µm diameter.

The use of solid–liquid phase change to achieve change of state in extrusion freeforming of ceramics is not suitable for fine work because the filament solidifies too quickly in ambient air. Thus fine log-pile structures can be produced with 100 µm dia. filament but not with 76 µm filament. The use of polymerisation as a method of state-change has been described by others and the present work points to the potential for controlled drying offered by solvent-based systems. The contact area of welds that formed at junctions was small and the filaments deformed little. When a wall was made, the surface ripples were pronounced but this does not matter in the creation of latticework. We suggest, on the basis of this work that extrusion freeforming provides a method for the construction of bone substitute material and of preforms for metal matrix composites.

#### Acknowledgements

The authors are grateful to the International Association for the Exchange of Students for Technical Experience (I.A.E.S.T.E) for arranging a summer placement for Imen Grida. We thank Mike Beasley at Parker Hannifin for help with programming the three-axis table and Bob Whitenstall for help with microscopy.

#### References

- Bourriau, J., Pottery from the Nile Valley before the Arab Conquest. *Cambridge University Press*, 15–18.
- Crump, S., Fused deposition modelling (FDM): putting rapid back in prototyping. *Proc. 2nd Int. Conf. on Rapid Prototyping*, 358–361.
- Zhong, W. H., Li, F., Zhang, Z. G., Song, L. L. and Li, Z. M., Short fibre reinforced composites for fused deposition modelling. *Materials Science and Engineering A—Structural Materials Properties Microstructure and Processing*, 2001, **301**, 125–130.
- Gray, R. W., Baird, D. G. and Bohn, J. H., Thermoplastic composites reinforced with long fiber thermotropic liquid crystalline polymers for fused deposition modelling. *Polymer Composites*, 1998, **19**, 383–394.
- Dao, Q., Frimodig, J. C., Le, H. N., Li, X. Z., Putnam, S. B., Golda, K., Foyos, J., Noorani, R. and Fritz, B., Calculation of shrinkage compensation factors for rapid prototyping (FDM). *Computer Applications in Engineering Education*, 1999, **1650**, 7186–195.
- Masood, S. H., Rattanawong, W. and Lovenitti, P., Part build orientations based on volumetric error in FDM. *Int. J. Adv. Manuf. Technol.*, 2000, **16**, 162–168.
- Ziemian, C. W. and Crown, P. M., Computer aided decision support for fused deposition modelling. *Rapid Prototyping Journal*, 2001, **7**, 138–147.
- Kulkarni, P. and Dutta, D., Deposition strategies and resulting part stiffnesses in fused deposition modelling. *Journal of Manufacturing Science and Engineering-Transactions of the ASME*, 1999, **121**, 93–103.
- Geiger, M., Steger, W., Greul, M. and Sindel, M., Multiphase jet solidification. *EARP Newsletter 3*, Aarhus 1994.
- Greul, M., Pintant, T. and Greulich, M., Rapid prototyping of functional metallic parts. *Computers in Industry*, 1995, **28**, 23–28.
- Greul, M. and Lenk, R., Near-net-shape ceramic and composite parts by multiphase jet solidification (MJS). *Industrial Ceramics*, 2000, **20**, 115–117.
- Lenk, R., Rapid prototyping of ceramic components. *Advanced Engineering Materials*, 2000, **2**, 40.
- Agarwala, M. K., Bandyopadhyay, A., van Weeren, R., Safari, A., Danforth, S. C., Langrana, N. A., Jamalabad, V. R. and Whalen, P. J., FDC, rapid fabrication of structural components. *American Ceramic Society Bulletin*, 1996, **75**, 60–65.
- Lous, G. M., Cornejo, I. A., McNulty, T. F., Safari, A. and Danforth, S. C., Fabrication of piezoelectric ceramic/polymer composite transducers using fused deposition of ceramics. *Journal of the American Ceramic Society*, 2000, **83**, 124–128.
- Bandyopadhyay, A., Panda, R. K., Janas, V. E., Agarwala, M. K., Danforth, S. C. and Safari, A., Processing of piezocomposites by fused deposition techniques. *Journal of the American Ceramic Society*, 1997, **80**, 1366–1372.
- Rangarajan, S., Qu, G., Venkataraman, N., Safari, A. and Danforth, S. C., Powder Processing, rheology, and mechanical properties of feedstock for fused deposition of Si<sub>3</sub>N<sub>4</sub> ceramics. *Journal of the American Ceramic Society*, 2000, **83**, 1663–1669.
- Chen, Y., Bartzos, D., Lu, Y., Niver, E., Pilleux, M. E., Allahverdi, M., Danforth, S. C. and Safari, A., Simulation, fabrication and characterisation of 3-D alumina photonic bandgap structures. *Microwave and Optical Technology Letters*, 2001, **30**, 305–307.
- Allahverdi, M., Danforth, S. C., Jafari, M. and Safari, A., Processing of advanced electroceramic components by fused deposition technique. *Journal of the European Ceramic Society*, 2001, **21**, 1485–1490.
- Vaidyanathan, R., Walish, J., Lombardi, J. L., Kasichainula, S., Calvert, P. and Cooper, K. C., The extrusion freeforming of functional ceramic prototypes. *JoM—Journal of the Minerals Metals and Materials Society*, 2000, **52**, 34–37.
- Lombardi, J. L. and Calvert, P., Extrusion freeforming of Nylon 6 materials. *Polymer*, 1999, **40**, 1775–1779.
- Tyberg, J. and Bohn, J. H., FDM systems and local and adaptive slicing. *Materials and Design*, 1999, **20**, 77–82.
- Zerbo, I. R., Bronckers, A. L. J. J., de Lange, G. L., van Beek, G. J. and Burger, E. H., Histology of human alveolar bone regeneration with a porous tricalcium phosphate—a report of two cases. *Clinical Oral Implants Research*, 2001, **12**, 379–384.
- Schwartz, C., Liss, P., Jacquemaire, B., Lecestre, P. and Frayssinet, P., Biphasic synthetic bone substitute use in orthopaedic and trauma surgery: clinical, radiological and histological results. *Journal of Materials Science — Materials in Medicine*, 1999, **10**, 821–825.
- Peng, H. X., Fan, Z. and Evans, J. R. G., Bi-continuous metal matrix composites. *Mater. Sci. Eng.*, 2001, **A303**, 37–45.
- Peng, H. X., Fan, Z. and Evans, J. R. G., Cellular arrays of alumina fibres. *J. Mater. Sci.*, 2001, **36**, 1007–1013.
- Peng, H. X., Fan, Z. and Evans, J. R. G., Novel MMC microstructure with tailored distribution of the reinforcing phase. *J. Microscopy*, 2001, **201**, 333–338.

27. Peng, H. X., Fan, Z., Mudher, D. S. and Evans, J. R. G., Microstructures and mechanical properties of engineered short fibre reinforced aluminium matrix composites. *Mater. Sci. Eng. A*, in press.
28. Hutmacher, D. W., Zein, I. and Teoh, S. H., Processing of bioresorbable scaffolds for tissue engineering of bone by applying rapid prototyping technologies. In *Processing and Fabrication of Advanced Materials VIII*, ed. K. A. Khor, T. S. Srivatsan, M. Wang, W. Zhou and F. Boey. World Scientific Publ., Singapore, 2000, pp. 201–206.
29. Hutmacher, D. W., Schantz, T., Zein, I., Ng, K. W., Teoh, S. H. and Tan, K. C., Mechanical properties and cell cultural response of polycaprolactone scaffolds designed and fabricated via fused deposition modelling. *Journal of Biomedical Materials Research*, 2001, **55**, 203–216.
30. Song, J. H. and Evans, J. R. G., The injection moulding of fine and ultrafine zirconia powders. *Ceram. Int.*, 1995, **21**, 325–333.
31. Song, J. H. and Evans, J. R. G., Ultrafine ceramic powder injection moulding: the role of dispersants. *J. Rheol.*, 1996, **40**, 131–152.
32. Barnes, H. A., A review of the slip (wall depletion) of polymer solutions, emulsions and particle suspensions in viscometers: its cause, character and cure. *J. Non-Newtonian Fluid Mech.*, 1995, **56**, 221–251.
33. Gauthier, F., Goldsmith, H. L. and Manson, *Trans. Soc. Rheol.*, 1971, **15**, 297–330.
34. Cogswell, F. N., *Polymer Melt Rheology*. Goodwin, London, 1981, pp. 141–142.
35. Hess, W. M., Characterisation of dispersions. *Rubb. Chem. Technol.*, 1991, **64**, 386–449.
36. Zhang, T. and Evans, J. R. G., Predicting the viscosity of ceramic injection moulding suspensions. *J. Eur. Ceram. Soc.*, 1989, **5**, 165–172.
37. Zhang, T., Evans, J. R. G. and Dutta, K. K., Thermal properties of ceramic injection moulding suspensions in the liquid and solid states. *J. Eur. Ceram. Soc.*, 1989, **5**, 303–309.
38. Coulson, J. M. and Richardson, J. F., *Chemical Engineering, Volume 1: Fluid Flow, Heat Transfer and Mass Transfer*, 5th edn. Butterworth-Heinemann, Oxford, 1997 p. 386.
39. Heisler, M. P., Temperature charts for induction and constant temperature heating. *Trans. ASME*, 227–236.